Impact of Rogowski Sensors on the EMC Performance of Medium Voltage Power Substations

Christian Suttner*, Stefan Tenbohlen
Institute of Power Transmission and High Voltage Technology (IEH), University of Stuttgart
Stuttgart, Germany
*christian.suttner@ieh.uni-stuttgart.de

Werner Ebbinghaus
ABB AG –
PPMV-E
Ratingen, Germany
werner.d.ebbinghaus@de.abb.com

***Abstract*— The application of Rogowski sensors in protection and control equipment has many benefits compared to traditional instrument transformers. However, the signal levels of these sensors are small compared to possible disturbances, which raises questions regarding the immunity of such applications to switching transients. This contribution investigates a protection application with Rogowski sensors from the EMC point of view. Therefore, the disturbances that are generated by the primary parts of the switchgear are described. The propagation path of the interference is presented and differences to conventional applications are discussed. The effectiveness of different EMC measures is evaluated, based on the disturbance voltages occurring at the input terminals of the protection device.**

Keywords*— Rogowski coil; transients; EMC; current sensor; low power instrument transformer; medium voltage; switchgear

I. Introduction

Intelligent electronic devices (IEDs) are used for measurement, monitoring and protection applications in medium voltage switchgear. For this purpose, an accurate measurement of both the nominal current (e.g. 1.25 kA) and the fault current (e.g. 50 kA) is required. The principle of a conventional current transformer (CT) is an iron core with a secondary winding, placed on the primary conductor, according to Figure 1a. Due to the nonlinear magnetization characteristic of the core, the accuracy is limited to a certain range of the primary current and the burden. Separate units are used with multiple CT cores, or even multiple CTs may be necessary, in order to cover the protection and the metering functionality with the accuracy demanded. The complex CT calculations for high-end protection solutions often require extensive research of network parameters and result in more than 100 different CT types for one type of switchgear. The transmission ratios have to be defined in advance, with no flexibility of changing the application conditions later on. The ability of CTs to provide enough output power to drive electromagnetic relays is not needed for modern IEDs. The formerly important burden of the secondary wiring is almost eliminated, due to digital field bus technology. The large dimensions and the heat dissipation of the CTs in gas-insulated switchgear keeps manufacturers from designing smaller gas compartments. Modern secondary equipment and communication standards open up the possibility of using new designs and technologies, such as low power current transformers and Rogowski sensors.

Rogowski sensors, as shown in Figure 1b, are classified as electronic instrument transformers and defined by the IEC standard 60044-8 [1]. They do not have a ferromagnetic core, are not prone to any saturation effects and can, therefore, provide an accurate image of the primary current in a much wider range. The accuracy limit factor [1] is up to 30 times higher than for a conventional CT.

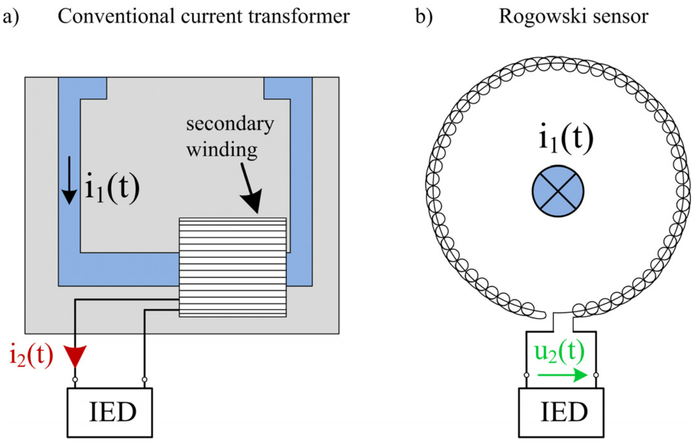

Fig. 1. Schematic structure of conventional CT and Rogowski coil.

Due to the increasing share of renewable energy sources in distribution grids, a sufficient number of measuring points is needed to retain control of the load flows. Since Rogowski sensors can be produced at low cost and require only a little installation space, they are ideally suited for upgrading existing substations and ring main units with a current measurement.

It is especially important to prevent the unintended operation of protection functions, caused by switching transients of the switchgear itself, for the consideration of the EMC performance of substations. Thus, section II describes the working principle of Rogowski coils and highlights the problem caused by transient overvoltages in combination with low signal levels which arises and the necessity of signal processing. The characteristics of the transients which occur are described in section III. Subsequently, section IV presents the disturbance propagation paths of the Rogowski sensor and the conventional CT. The differential mode coupling in the Rogowski sensor is illustrated by a simulation model in section V, and the impact factors on common mode coupling are shown by measurements in section VI.

II. CURRENT MEASUREMENT WITH ROGOWSKI SENSORS

Whereas the secondary current $i_2(t)$ corresponds directly to the primary current $i_1(t)$ in a conventional CT, the Rogowski sensor provides an output voltage $u_2(t)$ which is a scaled time derivative of the primary current. This results in a phase shift of 90° for harmonic currents. An accurate image of the original input current can be obtained by performing an integration of the signal. In order to minimize the influence of external magnetic fields, the winding wire is returned to the starting point along the central axis of the winding (see Figure 1b).

The amplitude of the secondary voltage is proportional to the dimensions of the secondary winding, and to the rate of current change. Excluding the burden, the following equation applies [2]:

$$\mathrm{u}_2(\mathrm{t}) = \mu_0 \cdot n \cdot A_c \frac{di_1(t)}{dt} = -M_{12} \cdot \frac{di_1(t)}{dt} \tag{1}$$

where:
- μ_0 is the permeability of vacuum
- n is the number of turns
- A_C is the cross section of the nonmagnetic core
- M_{12} is the mutual inductance

The output level of Rogowski sensors commercially available is rather small, e.g. transmission ratio 0.15 V/80 A. Therefore, the amplitude of the output voltage at a primary current of 1250 A is 2.34 V. Practical experiences show that, without proper EMC measures, the disturbance voltages at the high impedance input of the IED can regularly exceed 10 V. From the EMC point of view, the integration of the sensor signal mentioned previously becomes a problem, as interference voltages are coupled onto the signal lines of the sensor. The high disturbance voltages are out of the range of the analog input of the IED. Due to the integration of the signal, a faulty measurement sample is not discarded and the sensor input can encounter offset errors. The typical dynamic range of an IED's internal analog to digital converter (ADC) is ±10 V.

The following example illustrates what happens if a pulse with high amplitude causes a corrupted measurement sample at the maximum value of the ADC's dynamic range: Assuming a sampling frequency of 20 kHz, the sampled signal looks as shown in Figure 2.

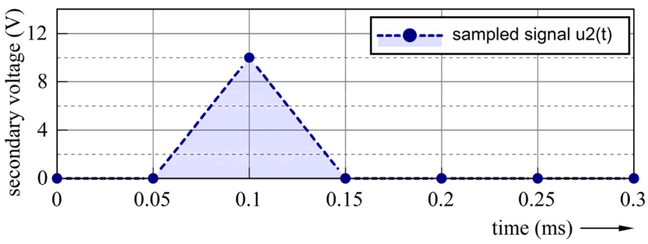

Fig. 2. Sampled disturbance signal at the IED input.

The sampled signal contains a single faulty measurement sample occurring at 0.1 ms. There is no actual operating current, therefore, all other samples in the figure are zero. In the case of a Rogowski sensor, this signal will be integrated to obtain the $\mathrm{i}_1(\mathrm{t})$ signal. The voltage/time area calculated below the curve causes a DC offset in the current signal. The amplitude of the DC offset can be calculated according to Equation 2.

$$\mathrm{I}_1(\mathrm{t}) = \frac{1}{M_{12}} \cdot \int \mathrm{u}_2(t)dt \tag{2}$$

Such DC offsets caused by switching transients are expected to be critical due to starting or tripping various protection functions. The unambiguous identification of corrupted measurements is a great challenge for the protection equipment, because they have to be instantaneously distinguished from fully displaced short-circuit currents. Although modern IEDs can handle single measurement errors, the probability of interference increases with the duration of the disturbance. Therefore, it is important that the current sensor inputs are protected from interferences, e.g. by proper shielding.

III. ORIGIN OF SWITCHING TRANSIENTS

Switching transients are originated by arcing phenomena during switching operations. The arcing itself is characterized by the functional principle of the switch. The probability of occurrence and the correlating EMC stress of restrikes for typical vacuum circuit breakers (CB) depend primarily on the load. However, single prestrikes at the CB contacts can also be found during any closing operation, independent of the load condition [3].

There are always small capacitive stray loads C_{stray} with values of a few tens of picofarads up to nanofarads during the disconnector operation (see Figure 3) [6]. They consist of the capacitances of the switchgear and connected power cables, in the case of special bus coupler panels [7].

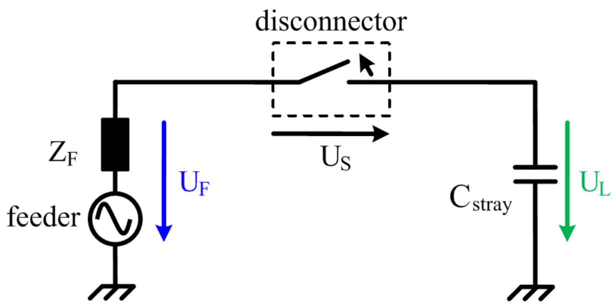

Fig. 3. Equivalent circuit diagram of a disconnector opening operation.

Practical experiences prove the theory that moving disconnectors within bus coupler panels (both transverse and longitudinal) generate the most severe EM disturbances. The disconnection of a busbar coupling is assumed to be the disturbance source for the following considerations. Figure 4 shows the voltage signals on both sides of the disconnector, according to the equivalent circuit diagram of Figure 3.

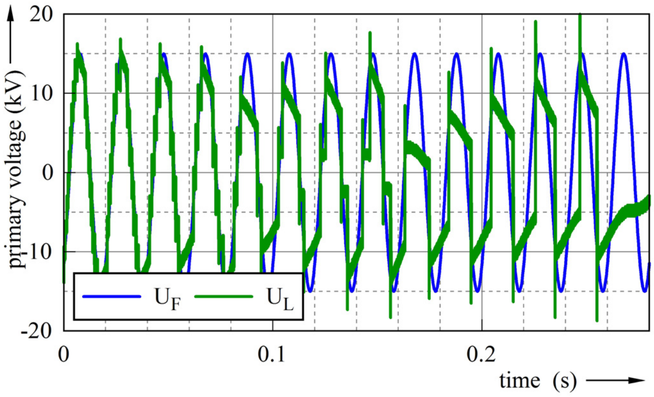

Fig. 4. Voltages during disconnector opening in a bus coupler panel.

According to [4], each recharging process of the parasitic capacitance C_{stray} generates two travelling waves of inverse polarity on the primary conductors, one in each direction. The travelling waves potentially cause conducted disturbances in all devices connected to the primary parts, such as voltage indicators or IEDs. The amplitude of the transient overvoltages at the IED is linearly dependent on the rise in time and the peak value of the wave front at the primary terminals of the instrument transformer. The amplitude of the transient disturbance at the analog measurement inputs of the IED is primarily related to:

- the operating voltage of the switchgear

  A higher operating voltage leads to higher ignition voltages at the switch contacts, higher wave fronts and higher disturbance amplitudes. In the worst case of a breaking operation, the maximum expected ignition voltage is twice the peak value of the line-to-earth voltage applied [5].

- the type of switchgear panel

  Practical experiences at different sites have shown that bus coupler panels generate the most severe disturbances. Feeder panels are less critical to self-interference. Their CB is usually open during the disconnector breaking operation. Therefore, the instrument transformer is galvanically isolated from the busbar parts carrying the ignition voltage.

- the insulating medium of the disconnector

  A higher breakdown field strength of the insulation medium generally causes steeper wave fronts and, thus, more spectral components at higher frequencies. Nevertheless, more detailed investigations have shown only small differences between air and SF_6 insulated disconnectors (see Figure 5). The rise times of the travelling waves measured at the current transformer's primary clamps have almost the same value of about 15 ns. The reason for this unexpectedly small deviation could be the poor wave propagation characteristics of the panel at higher frequencies.

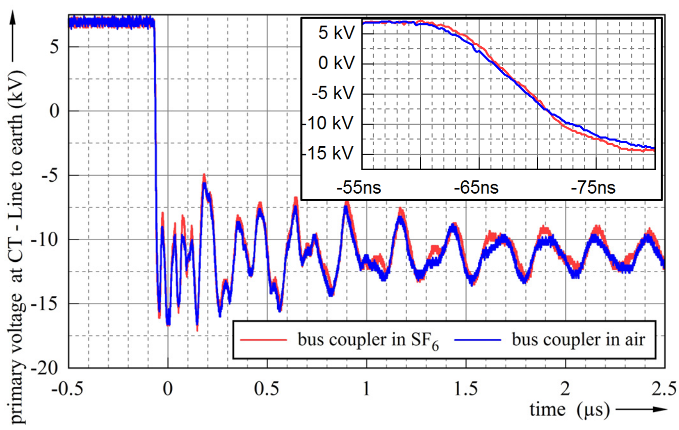

Fig. 5. Comparison of the wave front characteristics due to ignitions at disconnector contacts in air and SF_6.

IV. DISTURBANCE PROPAGATION PATHS

A. Conventional current transformers

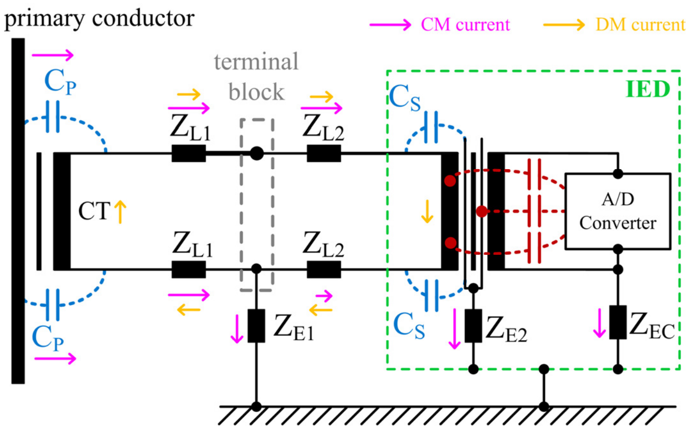

Fig. 6. Disturbance propagation on the primary and secondary parts of a typical switchgear panel.

The secondary wiring in conventional CT applications consists of unshielded single wires. The disturbance propagation is mostly capacitive via the stray capacitance C_P. The common mode coupling, indicated by arrows in Figure 6, is influenced by:

- the coupling capacitance C_P

  The value of C_P in a standard type CT is usually in the range of picofarads. Specially shielded transformers with a lower C_P may be applied at voltage levels exceeding 36 kV. A high coupling capacitance causes stronger coupling, which results in higher disturbance voltages at the IED inputs.

- the length, respectively, inductance ratios of signal wires

  The secondary wiring in conventional CT applications is commonly grounded in one central spot in the low voltage compartment to avoid high current injection in case of a short circuit; see terminal block in Figure 6. Assuming that the secondary wires can be described as transmission lines, a variation of the line lengths changes the impedance conditions of the system essentially. Changing impedances leads to different disturbance voltage distributions.

- the IED input impedance

  The secondary transformer inside the IED is usually shielded to protect the ADC from conducted interference. In the case of high frequency common mode disturbances, the IED input impedance is mostly determined by the inductive component of Z_{E2}.

Because the reference potential for the ADC is the signal ground inside the IED, the ground impedance of the IED housing is irrelevant to the disturbance at the input and is, therefore, not shown in Figures 6 and 7.

B. *Rogowski coil*

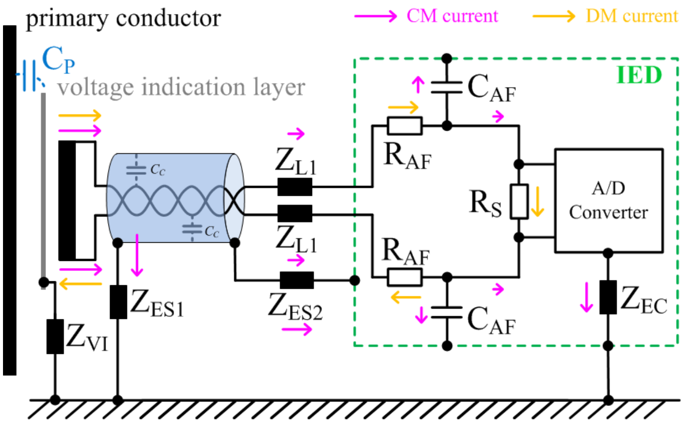

Fig. 7. Disturbance propagation in a sensor application

The secondary wiring in Rogowski sensor applications is implemented as shielded twisted pair cables. The common mode propagation is determined by:

- the coupling capacitance C_P and impedance Z_{VI}

  Due to the smaller dimensions of the sensor, the stray capacitance to the busbar is much lower than in a conventional CT. Additionally, the Rogowski coils are mostly applied onto bushings, containing coupling layers for voltage indication. This creates a shielding effect which eliminates the stray capacitance almost completely. However, the inductive part of the impedance Z_{VI} becomes more critical for high frequencies, so that a small common mode current is still coupled into the sensor wiring.

- the shielded signal cable

  According to the standard [1], a shielding is required for the signal cable. The shielding affects the disturbance voltage by providing a capacitive bypass C_C to the ground. The ground impedances Z_{ES1} and Z_{ES2} of that shield are limiting its effectiveness at high frequencies.

- the IED input impedance

  Because the output power of the sensors is limited, the impedance of the analog sensor input has to be high. Consequently, for high frequency common mode disturbances, the input impedance of the IED is primarily defined by the low pass filters of the analog input circuit. The cut-off frequency of such filters is usually more than 5 kHz.

V. Differential Mode Coupling in Rogowski Coils

The fact that the output voltage of the sensor refers to the time derivative of the primary current in Rogowski coil applications suggests that the output voltage rises when the frequency of the input signal is increased. Because switching disturbances contain high frequency components, the resulting output voltage could be very high. A simulation model of the Rogowski coil investigated, according to the equivalent circuit diagram in Figure 8, was created to evaluate the danger of high differential voltages caused by inductive coupling.

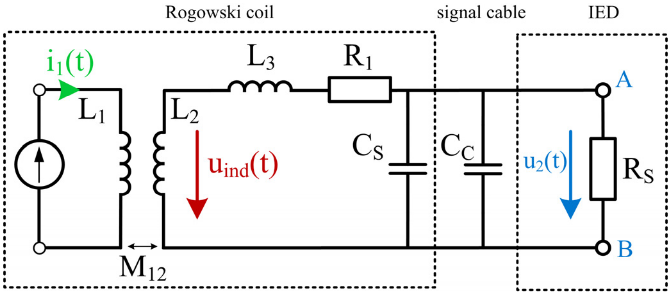

Fig. 8. Simplified equivalent circuit of sensor and burden

The mutual inductance M_{12} between the primary conductor and the winding wire can be calculated by using the rated values of the sensor ($i_{1r} = 80$ A; $u_{2r} = 150$ mV):

$$i_1(t) = \hat{I}_1(t) \cdot \sin(\omega t) \tag{3}$$

$$\left.\frac{di_{1r}}{dt}\right|_{max} = \hat{I}_{1r} \cdot \omega = 80\,\mathrm{A} \cdot \sqrt{2} \cdot \omega = 35525 \frac{\mathrm{A}}{\mathrm{s}} \tag{4}$$

The current change rate of (4) inserted in Equation (1) gives:

$$M_{12} = \frac{u_{2r}|_{max}}{\left.\frac{di_{1r}}{dt}\right|_{max}} = \frac{150\,\mathrm{mV} \cdot \sqrt{2}}{35525\,\frac{\mathrm{A}}{\mathrm{s}}} \approx 6\,\mu\mathrm{H} \tag{5}$$

The values for the elements L_3 (438.4 mH), R_1 (2.8 kΩ) and C_S (22 pF) have been measured with an impedance analyzer. The differential input impedance of the IED is 1.2 MΩ.

Figure 9 shows the result of the differential mode disturbance simulation using the simplified equivalent circuit of the sensor, presented in Figure 8. There is a double exponential impulse current on the primary conductor with a peak value of 25 A, a rise time of 10 ns and a time to half value of 500 ns. The resulting secondary output voltage $u_2(t)$ has the shape of a damped oscillatory wave with a resonance frequency of 18 kHz and a peak amplitude of 180 mV. Due to the capacitance between the secondary windings C_S and the cable capacitance C_C in between the twisted signal lines, the amplitude of $u_2(t)$ is much lower than the voltage $u_{ind}(t)$ induced originally. It is within the range of volts and, therefore, does not exceed the dynamic range of the ADC.

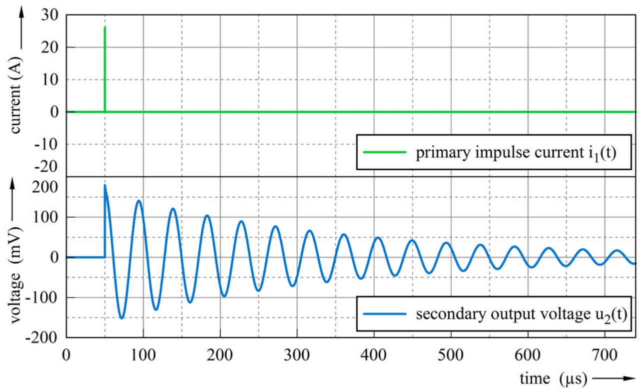

Fig. 9. Simulated differential mode disturbance

The frequency dependent output voltage of the Rogowski coil is shown in Figure 10. It can be seen that the output voltage increases at a rate of 20 dB/decade up to the resonance frequency. The stray capacitances C_S and C_P dominate the response (output voltage u_{out_s}) in higher frequencies. This explains the low secondary voltage despite the steep current edge on the busbar.

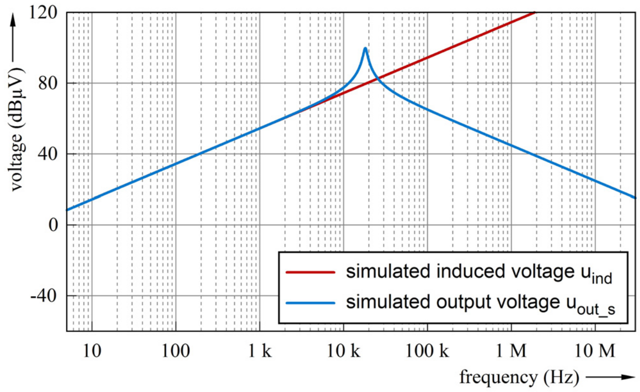

Fig. 10. Output voltage of the Rogowski coil at 80 A (rated current)

Because of the high impedance of the input, the function does not become flat. The resonance frequency is determined by the sum of C_S and C_C, as well as by the inductance L_3. Whereas the inductance is determined by the application, there is some flexibility for designers to increase the capacitance C_S in order to shift the resonance peak to lower frequencies. This would result in even lower differential disturbances and minimize the risk of measurement error.

VI. Common Mode Disturbance Measurements

A laboratory test setup was created in order to investigate the common mode disturbance voltage at the input terminals of the IED (see Figure 11): The Rogowski sensor was placed onto a bushing to accurately reproduce the coupling path inside the actual switchgear. The signal cable was routed at the height of 20 cm above a ground plane. The conductor inside the bushing was excited with an electrostatic discharge (ESD). The disturbance voltage between the signal line and ground was measured at the equivalent impedance.

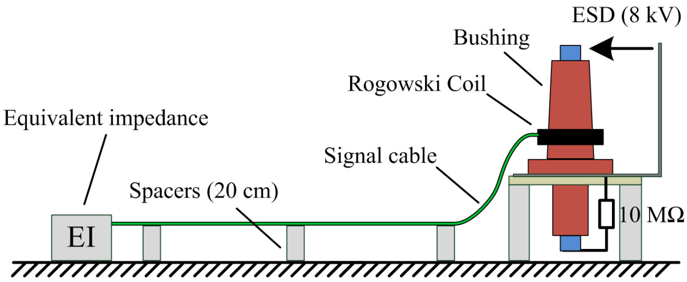

Fig. 11. Laboratory setup for ESD testing

A. Effect of shielded signal cable

The screen of the signal cable provides a stray capacitance to ground in the range of 100 pF. Two different signal cables are compared regarding the disturbance voltage at the current sensor input of the IED in Figure 12.

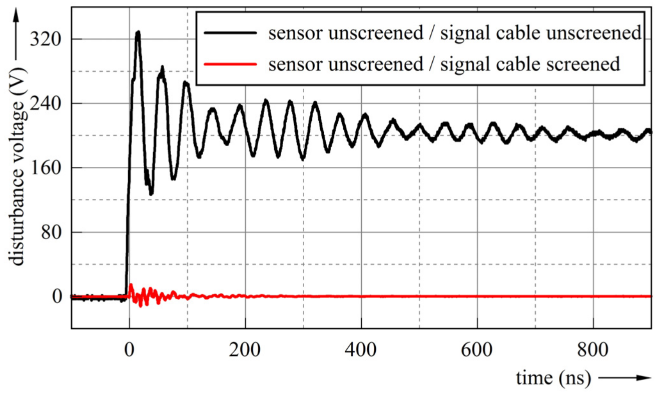

Fig. 12. Common mode disturbance voltage at IED input terminal with shielded and unshielded signal cable

Because of the high impedance of the IED input, the capacitive bypass provided by the shield reduces the disturbance voltage considerably. There can be transient currents with peak values of up to 40 A on the cable shield in a real disconnector operation. Therefore, the ground impedance Z_{ES}, as shown in Figure 6, affects the effectiveness of this shield [4].

B. Effect of sensor shielding

If it is assumed that the signal cable is already shielded, as required in the standard [1], the disturbance voltage can be further reduced by shielding the sensor itself. This shield needs to have a thin gap in the traverse axis in order to prevent eddy currents from distorting the signal.

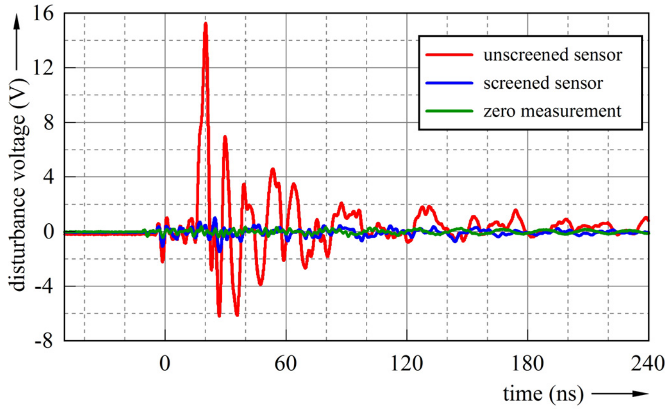

Fig. 13. Impact of sensor shielding on common mode disturbance voltage

The screening of the sensor reduces the interference at the input terminal to a level within the range of the zero measurement (see Figure 13). The zero measurement was performed with the sensor cable disconnected. The input terminals of the equivalent impedance were shorted and the busbar was excited with the ESD impulse. The small signal in the zero measurement is caused by capacitive near field coupling of the ESD into the measurement probe, which is connected to the equivalent impedance.

A similar shielding effect can be achieved by placing the sensor onto a bushing containing voltage indication layers. These provide a cylindrical capacitance to ground and inhibit the disturbance propagation by reducing the stray capacitance C_P, as is shown in Figure 7.

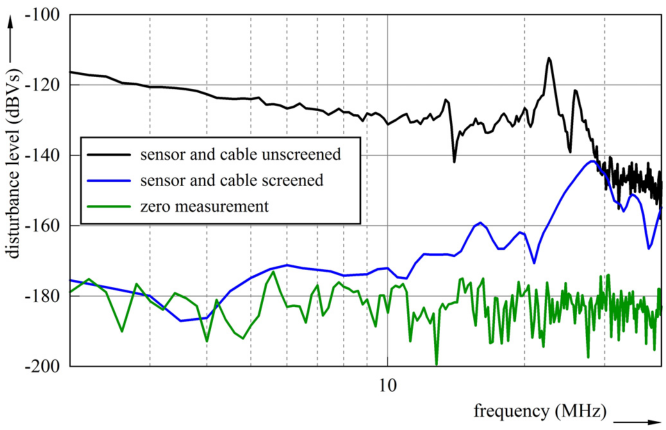

Fig. 14. Analysis of common mode disturbance in the frequency domain

As can be seen from Figure 14, the shielding effect decreases for higher frequencies. This is caused by the inductive part of the shield's ground impedance mentioned in section III. According to [7], disconnector arcing can stimulate frequencies up to 80 MHz. The shield of a standard cable with an RJ-45 connector on one side and a 20 cm pigtail on the other will only work effectively for up to 30 MHz. In switchgear with a high operating voltage, this limit can be moved further up by using high-end shield connections.

C. Low pass filters

In special applications with high operating voltages and inductively dominated loads, vacuum circuit breakers can stimulate frequencies even higher than 100 MHz. These disturbances can be effectively suppressed by low pass filters in the signal path. Such a filter is usually integrated into the analog input board of the IED, but it could also be placed in the sensor itself or within a signal splitter for protection testing purposes.

VII. CONCLUSION

The comparison of the analog measurement circuits of conventional CTs and Rogowski sensors has shown the advantages of the Rogowski application in disturbance mitigation. Differential mode disturbances, which may arise from steep current edges on the busbar, are limited by the stray components in the sensor and on the signal lines. The coupling efficiency of common mode disturbances can be significantly decreased by sensor shielding. Furthermore, the cable shields provide a capacitive bypass to disturbances which are already carried by the signal lines. However, this bypass is limited by the impedance associated with non-ideal grounding of the shields. Therefore, common mode currents remain the dominating source of interference. This has to be taken into account in the design of the sensor and the secondary wiring. Future studies will focus on the verification of the differential mode simulation by measurement. The motivation for performing a simulation in the first place was the effect of the network analyzers ground reference, which is not easy to circumvent.

REFERENCES

[1] IEC technical committee 38, 2002, "Instrument Transformers – Part 8: Electronic current transformers", International Standard IEC 60044-8 Edition 1.02.

[2] IEEE Power System Relaying Committee, 2007, "IEEE Guide for the Application of Rogowski Coils Used for Protective Relaying Purposes", IEEE Std C37.235-2007.

[3] Edgar Dullni, Wenkai Shang, Dietmar Gentsch, Ingmar Kleberg, Kaveh Niayesh, 2006, "Switching of Capacitive Currents and the Correlation of Restrike and Pre-ignition Behavior", Dielectrics and Electrical Insulation, IEEE Transactions on, Volume: 13, pp. 65-71.

[4] C.R. Paul, 1992, Introduction to Electromagnetic Compatibility, New York: John Wiley & Sons Inc.

[5] Adolf J. Schwab, Wolfgang Kürner, 2007, Elektromagnetische Verträglichkeit, Berlin / Heidelberg, Germany: Springer, pp. 88-91.

[6] Hugh M. Ryan, 2001, High Voltage Engineering & Testing, Stevenage, Institution of Engineering and Technology.

[7] Dennis Burger, Werner Ebbinghaus, 2011, "Sources of transient electromagnetic disturbance in medium voltage switchgear", EMC Europe 2011, York.